STUDIES ON WEAR BEHAVIOR OF ALUMINIUM-TIN ALLOY

A thesis submitted in partial fulfilment of the requirements for the degree of

Bachelor of technology

In

Metallurgical and Materials Engineering

By

SINDHOORA LAKSHMI PUVVADA (111MM0495)

AMIT KUMAR DAS (111MM0361)

UNDER THE GUIDANCE OF

Dr. SUBASH CHANDRA MISHRA

DEPARTMENT OF METALLURGICAL AND MATERIALS ENGINEERING

NATIONAL INSTITUTE OF TECHNOLOGY ROURKELA

2015

NATIONAL INSTITUTE OF TECHNOLOGY ROURKELA

CERTIFICATE

This is to certify that the thesis entitled "**STUDIES ON WEAR BEHAVIOR OF ALUMINIUM-TIN ALLOY**" submitted by SINDHOORA PUVVADA (111MM0495) and AMIT KUMAR DAS (111MM0361) in partial fulfillment of in partial fulfilment of the requirements for the award of BACHELOR OF TECHNOLOGY Degree in Metallurgical and Materials Engineering at the National Institute of Technology, Rourkela (Deemed University) is an authentic work carried out by him under my supervision and guidance.

To the best of my knowledge, the matter embodied in the thesis has not been submitted to any other University/ Institute for the award of any degree or diploma.

Date: 6th May, 2015

Prof. Dr. S.C.Mishra
Department of Metallurgical and Materials Engineering
NATIONAL INSTITUTE OF TECHNOLOGY ROURKELA

ACKNOWLEDGEMENT

It is an immense pleasure to express our deep sense of gratitude to **Prof. Subash Chandra Mishra** our guide and supervisor for his invaluable guidance, motivation and constant inspiration. We also express our sincere thanks to the Department of Metallurgical and Materials Engineering for all the help and coordination extended by the department.

We are also grateful to **Prof S.K. Acharya**, Department of Mechanical Engineering for his valuable time and cooperation for the completion of this work. We are greatly thankful to the staff members of the department, all our well-wishers, classmates and friends for their inspiration and help.

Date: 6th May, 2015

SINDHOORA LAKSHMI PUVVADA

(111MM0495)

Place: Rourkela

AMIT KUMAR DAS

(111MM0361)

ABSTRACT

Aluminum and its alloys offer substantial potential for industrial applications because of special characteristics like lightness, excellent resistance to atmospheric corrosion in marine, urban and industrial settings and their ability to be lend to a huge variety of surface treatments like anodization. Aluminium and Aluminium based alloys are used in the automotive industries, parts operated at severe wear and tear conditions. In the present work, with the objective of studying the wear behavior of Al-Sn alloys, some samples of Al and 1% Sn composition alloy were taken. The sliding wear behavior using ball on plate wear tester was observed. Erosion wear behavior, under the influence of different parameters like velocity and angle of incidence of silica particles, sand flux rate etc. was observed. Microstructural characterization, X- ray diffraction studies and surface properties after sliding wear test were also observed. In order to increase the life and performance of Aluminium alloys in various industrial sectors, tribological characterization is critical since failure from wear can be detrimental. Due to the significance associated with tribology, this particular alloy has been studied for tribological properties.

Variation of cumulative mass loss for different impingement angles were plotted and analyzed. The individual effects of control parameters was also observed. According to Taguchi analysis, of all the parameters affecting wear rate, “velocity” is the most significant parameter and angle of impingement plays a crucial role too. Corrosion behavior of Aluminium samples was also observed by immersing the Aluminium alloy samples in a sea water bath. Weight was taken after frequent intervals and thus material loss was determined from weight loss.

CONTENTS

List of Figures

List Of Tables

CHAPTER 1

Introduction

1.1. Research Background

Aluminium is the third most abundant metal and has become an economic competitor in engineering applications since the end of the nineteenth century. The most striking feature of Al is its versatility. This is due to the range of properties that can be developed from refined high purity Aluminium to most complex alloys of this metal.

Aluminium and its alloys are used extensively as materials in transportation (aerospace and automobiles), structural applications and engine components. Structural components made from Al and its alloys are important to aerospace industry. Thus it is necessary to study the tribological characteristics of Al and its alloys.

Interest in aluminum alloys was primarily due to the fact that a material having good sliding properties, which can withstand higher loads than the Babbitt's and thus allows to avoid loads of problems commonly encountered during both the manufacturing process and with the subsequent utilization of the copper-tin-lead and copper-lead alloys [1]. Al-Sn alloys have a very long history to be used as bearing materials. This is because these alloys offer a good combination of strength and surface properties. The homogenous and dispersed distribution of fine Sn which is lubrication phase in Al matrix is beneficial to friction and wear behavior. The wear properties of a few samples of Al and 1% Sn composition were studied here.

1.2. Why Aluminium?

The third most abundant element after oxygen and silicon is Aluminium. A broad variety of mechanical and physical properties can be procured from wrought Al. Some properties of this metal which are remarkable are:

1. The low density of Aluminium (which is $1/3^{rd}$ of that of steel) makes it possible to reduce weight of components and structures especially for applications like transport (aerospace prominently).

2. Ability to resist corrosion due to phenomenon of passivation. This is the formation of shielding oxide layer (Al_2O_3) which prevents the core from coming in direct contact with the environment.

3. This metal can easily be subjected to casting, drawing, extrusion and other forming processes.

4. Aluminium is remarkable for its electrical and thermal conductivity.

5. Aluminium is also useful due to its superconductivity in certain applications.

1.3 Why Aluminium Alloys?

Nomenclature of aluminium alloys are done as 4xxx, 5xxx and 6xxx series where the number represents the major alloying element. The properties of aluminium and its alloys that make them the most economically attractive for a wide variety of applications are:

- Al alloys have high specific modulus and high specific toughness, hence are used in automotive components for fuel saving and improving economy.

- Al alloys are of great use in electrical industry as thermal conductivity is twice that of Cu.

- Strength at low temperature: Brittle fracture problems do not occur with aluminum. As there is a decrease in temperature, the strength of Aluminium alloys increase without loss in quality making them particularly suitable for low temperature applications.

- Resilience under static and dynamic loading: Aluminium products behave elastically under static and dynamic loading conditions. Thus they have the ability to restore both shape and size. This is good when flexible strength is required.

- Ease of fabrication and machinability: It can be easily cast, rolled to any desired thickness (aluminium foils are so common), stamped, drawn, spun, forged and extruded to all shapes.

1.3.1 Aluminium–Tin Alloys

Tin has a low coefficient of friction, which is the first reason of it being used a as a bearing material. Tin is structurally weak. So when it is used bearing applications it is alloyed with copper and antimony to increase the hardness, tensile strength and fatigue resistance. The amount of tin in these alloys, called tin-base Babbitt's, is limited to 0.35 to 0.5% to avoid formation of the tin-lead eutectic that would significantly decrease strength properties at operating temperatures. Lead-base bearing alloys, called lead-base Babbitt's, include 12 to 18% antimony with 10% tin. In general, these alloys are inferior in strength to tin-base Babbitt's, and this must be equated with their lower cost.

In the automobile industry, Conventional Babbitt alloys, especially the lead bronzes are increasingly being replaced by aluminium alloys. The antiscoring and antifrictional properties of aluminium are enhanced by the addition of elements like tin or lead. There must be a balance between softness and strength in bearing alloys. Aluminum-tin bearing alloys represent an excellent compromise between the requirements for high fatigue strength and the need for good surface properties such as softness and seizure resistance. In general, homogenous and dispersed distribution of fine Sn which is lubrication phase in Al matrix is beneficial to friction and wear behavior. Aluminum-tin bearing alloys are usually employed in conjunction with hardened steel or ductile iron crankshafts and allow significantly higher loading than tin- or lead-base bearing alloys.

Low-tin aluminum-base alloys (5 to 7% Sn) containing small amounts of copper and nickel which as act as strengthening elements, are often used for connecting rods and thrust bearings in high-duty engines. Oil contamination should be avoided. Strict dimensional tolerances must be adhered to. Alloys containing 20 to 40% tin, remainder aluminum, show excellent resistance to corrosion by products of oil breakdown and good embeddability in dusty environments. The higher-tin alloys

contain adequate strength and better surface properties that make them useful for crosshead bearings in high-power marine diesel engines.

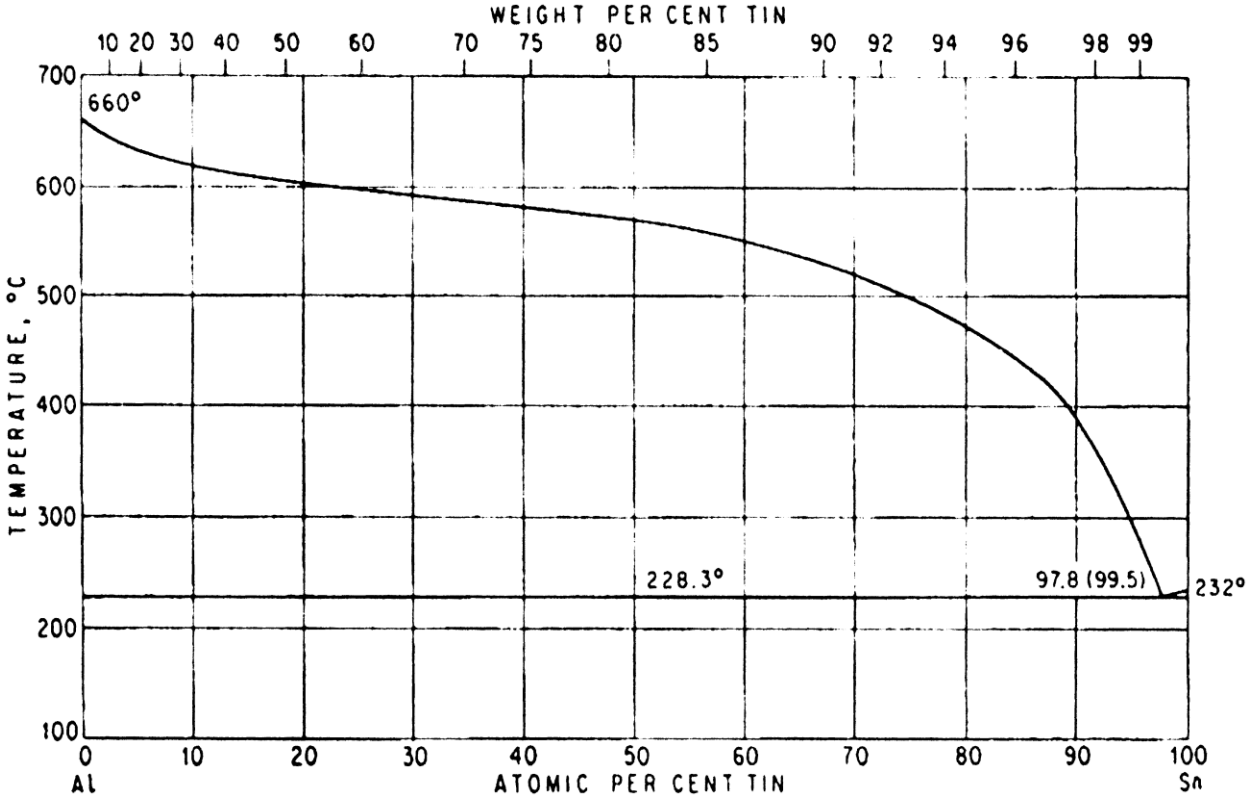

Fig 1: Phase diagram of Al-Sn alloy

Al – Sn alloys are completely miscible only above the liquidus line. In conventional casting, if such a homogeneous single phase liquid is cooled below the liquidus line, it transforms into two liquids i.e. aluminium rich and tin rich. The minor 'Sn' rich phase segregates out. If the homogeneous single Al-Sn liquid phase is rapidly cooled, the minor phase is disperses uniformly in aluminium rich matrix. Al – Sn is an immiscible binary alloy system with a solid solubility of Sn in Al below 0.09 wt. % at room temperature .The growing importance of Al – Sn based alloys as materials for engineering applications necessitates the development of uniform microstructures with improved performance.

According to the aluminum-tin equilibrium system, the solubility of tin in solid solution at 900 K is 0.1%, while at the eutectic temperature it goes down to the 0.005-0.07%. Tin with aluminum

forms a eutectic system at low eutectic temperature of 501-502 K and reveals a strong deviation of the eutectic point towards tin (99.5% Sn). Creating the bearing alloys structure on the aluminum-tin basis starts with the appearance of first crystals of solid solution out of super cooled liquid.

As a result of a low value of the phase distribution coefficient $k=C_S/C_L$ a diffusion of high quantities of tin admixture appears on a crystallization front. As the effect of crystallization the resultant appearance of concentration super-cooling becomes non-durable and tends to form cellular or dendritic surface. After the formation of cellular or dendritic crystals, the highly segregated eutectic liquid solidifies. As a result a net of developed dendritic crystallites with precipitates of the eutectic tin phase within inter-dendritic spaces appears in the structure of the alloy [2].

It follows from the above description of the aluminum-tin alloys solidifying process that an even distribution of the tin-rich eutectics in the cast material structure depends on a solution growth process. This implies that all parameters causing the grain refinement as well as the decrease of inter-dendritic distances will also be instrumental in making a more even distribution of tin.

Effective methods of grain refinement must be applied in the process of ingots production-original material for bimetallic bearing manufacturing-as well as such casting techniques that would allow for a faster solidifying process, so as to create the appropriate conditions for obtaining the correct structure.

Aluminium tin alloys have a wide miscibility gap in the molten state and are virtually insoluble in each other during solidification. Further difficulties comes into existence from the large freezing range of the alloys in addition with the with the wide density difference between the two components and immiscibility of Al-Sn system greatly increase the tin segregation or sedimentary tendency during alloy preparation. Therefore it has been difficult to introduce and uniformly disperse tin in Aluminium to the desired extent by conventional melting and casting techniques. Therefore, homogeneous distribution of Sn in Al matrix could not be easily obtained. Different preparing methods, including stir cast, rapid solid, physical vapor deposition, electro deposition,

powder metallurgy, severe plastic deformation, and mechanical alloying, have been used to enhance microstructure homogeneity and refine the size of Sn phase in Al – Sn alloys.
The existence of substantial differences in the respective specific weights of aluminum and tin poses the danger of gravity segregation in the metal bath during the melting stage and the preparation for casting. This phenomenon could effectively be minimized by the application of such melting method that would allow for the shortest possible melting time, and at the same time it would secure constant motion of the metal bath by way of moving the melting process into the induction crucible furnace. It is also very important to make sure that the ingot casting time is the shortest possible, so as to preclude the incidence of gravity segregation of the metal bath remaining in the crucible [3].

In internal combustion engines of automobiles, fatigue failure may sometimes occur in a short time when these alloys are used as bearing material, especially when the engines are operated continuously under heavy loads. This is because the temperature of the lubricant oil in an internal combustion engine becomes very high during the continuous full load running. For example, the temperature of the lubricant oil in an oil pan reaches 130ºC to 150ºC, so that the temperature of the sliding surface of the bearing is also raised very high. As a result, since the eutectic point of such an alloy is about 225ºC or so, the hardness of the alloy rapidly becomes low under the high temperature conditions causing the fusion and the migration of Sn component and the fatigue strength is resultantly lowered. In addition to the lowering of the fatigue strength due to the loss of hardness at high temperatures, the coarsening of tin particles in a conventional Al-Sn base alloy also causes lowering of the fatigue strength [1].

The reason why the content of tin is restricted to the range of 3.5 to 25 wt. % is that even though the addition of tin in an amount of more than 25 wt. % improves the conformability and low friction property, it slightly reduces the hardness of bearing alloy. When the alloy contains less than 3.5 wt. % tin, the bearing alloy becomes too hard and is insufficient in view of conformability, the addition quantity of tin is made small when a bearing receives a large load, much tin can be added to the bearing alloy for light duty purpose. However, in recent cases, the temperature of the bearing becomes often high due to the high temperature oil and this causes the deformation of the bearing which is followed by the occurrence of seizure and fatigue. Thus our main objectives through this

project are to study wear behavior of Al Sn alloys at a low Sn % (1 %) considering the present day industrial application [7].

During their use, these alloys are subjected to unproductive and harmful friction and continued impact by wind and erosive particles which leads to wear, material loss and damage to the structures. Wear leads to unwanted material losses and plays a very critical role in determining the life and suitability of the material for a particular application. Tribological studies concern with the study of wear, friction and lubrication of surfaces in motion relative to each other. Tribological characterization of Al Sn alloys is important for better life and performance in fields of tooling, aerospace and automobiles where catastrophic failures occur from friction and wear.

1.4 Hardness

Hardness is a characteristic of a material. It is defined as the resistance to indentation. By measuring the permanent depth of the indentation, hardness can be determined. For a fixed load and a given indenter, the smaller the indentation, the harder the material.

The Vickers test is more conveniently applicable than other hardness tests. And also the size of the indenter does not influence the calculations. The material's ability to resist plastic deformation is denoted by this number. The Vickers Pyramid Number (HV) is the unit of hardness given by the Vickers's hardness test.

When it is the case for small parts, thin sections, or case depth work, Vickers's hardness test method is used. The Vickers method is based on an Optical measurement system. The microhardness test procedure, ASTM E-384, specifies a range of light loads using a diamond indenter to make an indentation which is measured and thus converted to a hardness value. It is very useful for testing on a wide type of materials as long as test samples are carefully prepared. Here a square base pyramid shaped diamond indenter is used.

1.5 X- Ray Crystallography

X-ray crystallography is a tool used for identifying the atomic and molecular structure of a crystal, in which the crystalline atoms produces a beam of incident X-rays to diffract into many specific directions. The angles and intensities of these diffracted beams are measured, and thus the crystallographer can produce a 3D picture of the density of electrons within the crystal. The mean positions of the atoms in the crystal can be determined form the electron density. Besides their chemical bonds, their disorder and various other information can also be determined.

Single crystal X-ray diffraction can be considered to be the most precise method of X-ray crystallography. In this method, a beam of X-rays strike a single crystal which results into the production of scattered beams. The scattered beams make a diffraction pattern of spots when they fall on a piece of film or other detector. The values of the strengths and angles of these beams are recorded as crystal gradually rotates. Within the crystal, each spot is called a reflection as it corresponds to the reflection of X-rays from one set of evenly spaced planes. When crystals are of sufficient purity regularity and, X-ray diffraction data can determine the chemical bond lengths and angles to a few thousandths of an angstrom and to a within a few tenths of a degree, respectively.

Considering the incident X-rays 1 and 2 which are shown in the figure

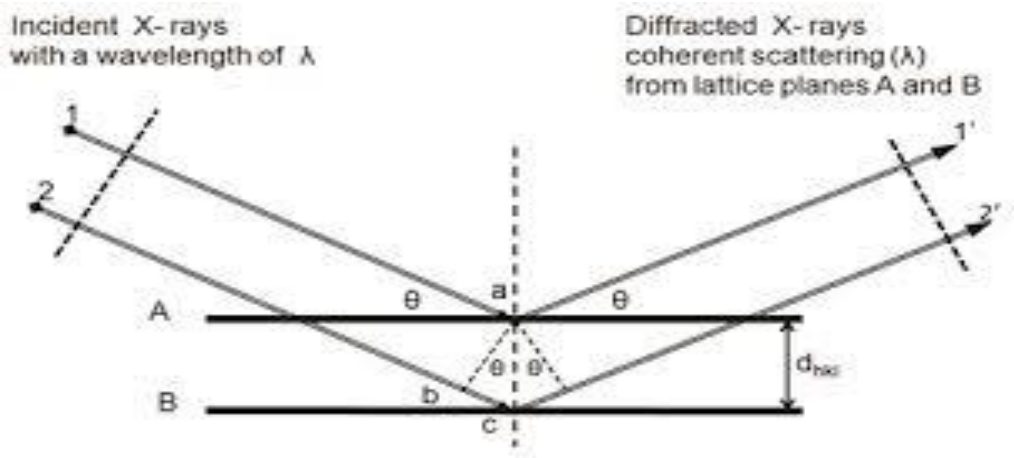

Fig 2: X-Ray Diffraction

- For the beams that are reflected to be in phase, the extra distance travelled by ray 2 (which is equal to AB +BC) must be an integral multiple of the wavelength λ. Thus, n λ = AB+BC, where n is considered to be the order of diffraction and is a positive integer.

- AB and BC are equal to dsinΘ, d being the interplanar spacing of the crystal planes with Miller indices (h k l).

- For constructive interference, n λ = 2dsinΘ, which is essential for the production of a diffraction peak of intense radiation.

- The necessary conditions of diffraction are given by this equation and it is called as Bragg's law.

1.6 Scanning Electron Microscope

A Scanning Electron Microscope (**SEM**) is a type of electron microscope that produces images of a sample by scanning it with a focused beam of electrons. The electrons and the atoms interact in the sample, which produces various signals that can be detected and that contain information about the sample's surface composition and topography. The electron beam is generally scanned in a raster scan pattern. The beam's position is combined with the detected signal to produce an image. SEM can achieve better than 1 nanometer resolution. Specimens can be observed in high as well as low vacuum, in wet conditions, and at a wide range of elevated or cryogenic temperatures [4].

The most common SEM mode is detection of secondary electrons emitted by atoms excited by the electron beam. The number of secondary electrons is dependent on the angle at which beam meets surface of specimen. Scanning the sample and collecting the secondary electrons with special detector will produce an image displaying the topography of the surface is created.

For traditional imaging in the SEM, samples must be electrically conductive, in any event at the surface, and electrically grounded to keep the amassing of electrostatic charge at the surface. Metal

items oblige minimal unique planning for SEM aside from cleaning and mounting on an sample stub. Nonconductive samples have a tendency to charge when examined by the electron shaft, and particularly in auxiliary electron imaging mode, this reasons examining shortcomings and other picture ancient rarities. They are hence typically covered with an ultrathin covering of electrically directing material, stored on the specimen either by low-vacuum sputter covering or by high-vacuum dissipation. Conductive materials in current utilization for sample covering incorporate gold, gold/palladium composite, platinum, osmium, iridium, tungsten, chromium, and graphite. Also, covering with substantial metals may expand sign/clamor proportion for tests of low nuclear number (Z). The change emerges on the grounds that auxiliary electron discharge for high-Z materials is upgraded.

A distinct option for covering for some natural specimens is to expand the mass conductivity of the material by impregnation with osmium utilizing variations of the OTO recoloring system (O-osmium, T-thio-carbohydrazide, and O-osmium).

Non-conducting samples may be imaged uncoated utilizing low voltage SEM operation. Environmental SEM instruments place the sample in a generally high-weight load where the working separation is short and the electron optical segment is differentially pumped to keep vacuum sufficiently low at the electron weapon. The high-weight locale around the specimen in the ESEM kills charge and gives an intensification of the optional electron signal. Low-voltage SEM is regularly led in a FEG-SEM on the grounds that the field outflow weapons (FEG) is equipped for delivering high essential electron splendor and little spot size even at low quickening possibilities. Working conditions to anticipate charging of non-conductive samples must be balanced such that the approaching pillar current was equivalent to aggregate of out coming auxiliary and backscattered electrons streams. It ordinarily happens at quickening voltages of 0.3–4 kV.

Fractograph is the investigation of cracked surfaces that could be possible on a light magnifying instrument or generally, on a SEM. The broke surface is decreased to a suitable size, cleaned of any natural deposits, and placed on a sample holder for review in the SEM. Metals, geographical samples, and incorporated circuits all may likewise be artificially cleaned for survey in the SEM.

1.7 Wear

It is characterized as a procedure of expulsion of material from one or both of two strong surfaces in strong contact. Wear is characterized as the harm to a strong surface, by and large including the dynamic loss of material, because of relative movement between two moving surfaces. Wear is not a natural material property but rather characteristics of the engineering system which rely on burden, speed, temperature, hardness, existence of outside material and the ecological conditions.

Wear is damage but it is not just limited to loss of material from surface but also by movement of material without loss of mass. An example is change of part dimension or geometry due to plastic deformation. Damage of a surface may also be caused due to a third mode which is development of cracks in a surface. Wear occurs mostly through interactions at the asperities on the surface.

Wear causes a very high annual expenditure by consumers and industry. In some industrial sectors like agriculture, wear causes replacement of about 40% of the components of equipment. It is estimated that 10% of all energy generated by man is dissipated in various friction processes. Hence, in an economic point of view minimization of wear is crucial.

Wear may be classified into two types:

- Single phase wear: when a solid moves relatively with respect to a sliding surface, material is removed from the surface. This may be due to sliding or rolling.
- Multi-phase wear: In this wear a solid, liquid or gas acts as a carrier for second phase which produces the wear.

1.7.1 Wear Mechanism

The common types of mechanisms of wear are as follows:

a. Abrasive wear
b. Sliding and Adhesive wear
c. Solid particle Erosion /Erosion wear

d. Fretting wear
e. Corrosive wear
f. Impact wear
g. Surface fatigue

1.7.1.1 Abrasive Wear

Abrasive wear may be defined as wear that occurs when a hard rough surface slides against and cuts grooves from a softer surface. Asperities or hard particles that cut grooves on rubbing surfaces produce abrasive wear. These hard particles may originate from any of the surfaces in contact. During sliding mechanisms, abrasion may originate from the already existing asperities of one surface (when it is harder than the other), wear fragments which after generation are continuously deformed and thus get work hardened or oxidized till they become harder than both the sliding surfaces or due to the penetration of hard particles from outside the system such as dirt. The properties of both the surfaces, their speed of contact, environmental conditions and presence of hard agents between the surfaces affects the rate of surface abrasion.

Several mechanisms have been proposed to explain abrasive wear. But no single mechanism is sufficient to explain all the loss. These mechanisms involve melting, fatigue and failure. They include plowing, wedge formation, cutting, micro-fatigue, and micro-cracking. Recent tribological surveys reveal that abrasive wear results in largest amount of loss in material during industrial practices.

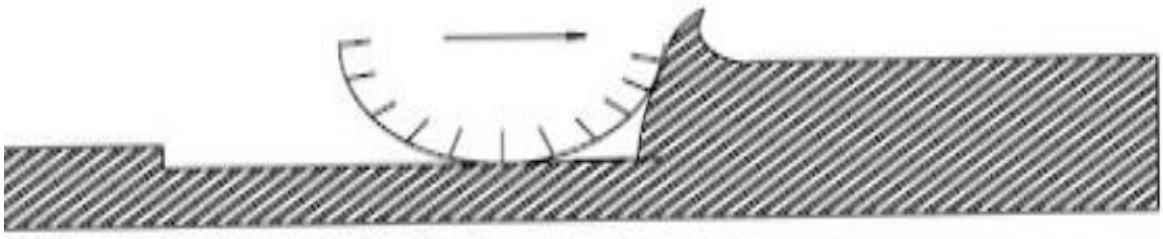

Fig 3: Schematic representation of Abrasion wear mechanism

1.7.1.2 Sliding and Adhesive Wear

Wear often occurs between solid surfaces in contact due to localized bonding resulting in exchange of material between the surfaces or loss from either surface.

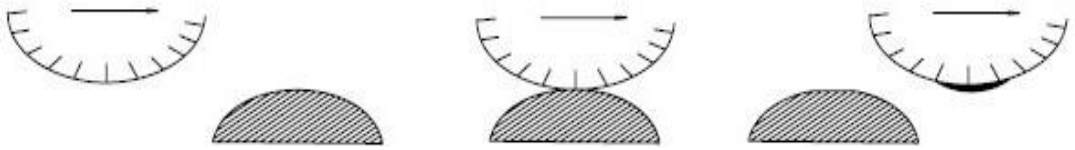

Fig 4: Schematic representation of Adhesive wear mechanism

For this type of wear to occur surfaces should be in intimate contact with each other and if they are held apart by oxide films, lubricating films, the tendency of abrasion decreases. Adhesive wear and sliding wear are not synonymous but adhesive wear may be called as sliding wear ambiguously. In this type of wear no particular agency can be attributed to as the cause of wear. When the intensity of sliding is greater than that in oxidation and fretting, adhesive wear is said to occur provided no abrasive substances are found [8].

1.7.1.3 Erosive Wear

Erosive wear can be defined as the process of metal removal due to impingement of solid particles on a surface. Erosion is caused by a gas or a liquid, which may or may not carry, entrained solid particles, impinging on a surface. When the angle of impingement is small, the wear produced is closely analogous to abrasion. When the angle of impingement is normal to the surface, material is displaced by plastic flow or is dislodged by brittle failure.

Fig 5: Schematic representation of Erosive wear mechanism

Solid particle erosion refers to a series of particles striking and rebounding from the surface, while abrasion results from the sliding of abrasive particles across a surface under the action of an externally applied force. During erosion, the force is exerted by the deceleration of particles on the material while in abrasion force is almost constant and is applied externally.

In erosion it has been established that the angle at which the stream impinges the surface influences the rate at which material removed from the surface and that this dependency is also influenced by the nature of wearing material.

Such a dependency is to be anticipated. This can be seen by considering the impact of a single particle with a surface. This angle determines the relative magnitude of the two velocity components of the impact, namely the component normal to the surface and the one parallel to the surface. The normal component will determine how long the impact will last i.e. the contact time, and the load. The product of contact time and the tangential velocity component determine the amount of sliding that takes place. The tangential velocity component also provides a shear loading to the surface, which is in addition to the normal load that the normal velocity component causes. Therefore as this angle changes, the amount of sliding that takes place also changes, as does the nature and magnitude of the stress system. Both of these aspects influence the way a material wears. These changes would also imply that different types of materials would exhibit different angular dependencies as well.

1.7.1.4 Fretting Wear

Fretting can be defined as the "small-amplitude oscillatory movement that may occur between contacting surfaces, which are usually at rest." Production of oxide debris is one of the immediate consequences of this phenomenon. The movement is due to external vibration. But in several cases, one of the members of the contact is subjected to a cyclic stress (fatigue). This gives rise to the initiation of fatigue cracks. This is called "fretting fatigue" or "contact fatigue.

1.7.1.5 Corrosive Wear

Most metals are thermodynamically unstable in air and react with oxygen to form an oxide, which usually develop layer or scales on the surface of metal or alloys when their interfacial bonds are poor. Corrosive wear is the gradual eating away or deterioration of unprotected metal surfaces by the effects of the atmosphere, acids, gases, alkalis, etc. This type of wear creates pits and perforations and may eventually dissolve metal parts. Wear is accompanied by corrosion in all environments except in inert atmospheres.

1.7.1.6 Impact Wear

It is defined as wear of a solid surface due to percussion. Percussion is a repetitive exposure to dynamic contact by another solid body. Several industries employ processes that lead to impact wear. Machine components, cams, and gears mate with a certain dynamic component. Typical applications occur in electromechanical printers; a prime example is that of typefaces, which are expected to hold definition, thus assuring high print quality, often for billions of cycles.

1.7.1.7 Surface Fatigue

Wear of a solid surface caused by fracture arising from material fatigue. The term ‘fatigue’ is broadly applied to the failure phenomenon where a solid is subjected to cyclic loading involving tension and compression above a certain critical stress. Repeated loading causes the generation of micro cracks, usually below the surface, at the site of a pre-existing point of weakness. On subsequent loading and unloading, the micro crack propagates. Once the crack reaches the critical size, it changes its direction to emerge at the surface, and thus flat sheet like particles is detached during wearing. The number of stress cycles required to cause such failure decreases as the corresponding magnitude of stress increases. Vibration is a common cause of fatigue wear. The schematic representation of the surface fatigue wear mechanism is shown in the diagram below.

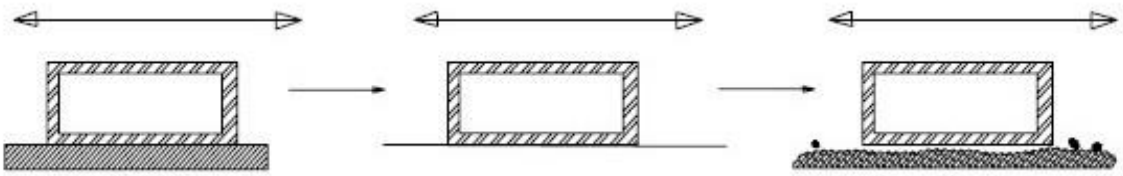

Fig 6: Schematic representation of Surface fatigue wear mechanism

1.8 Objectives of the present piece of investigation

The objectives of the present piece of investigation are as follows:

a) To calculate the cumulative mass loss of the Al-Sn alloy sample and determine the erosion wear rate. Also to relate the dependence of wear rate on parameters like impact angle, pressure etc.

b) To determine the sliding wear rate of the samples given and analyze the role of different parameters involved like track diameter, load applied and time of application of load.

c) To study the corrosion rate of the samples by determining the weight loss after stipulated time periods.

d) To observe the optical microstructure (light microscope) and measure the hardness (Vickers's hardness test).

e) To perform phase analysis of the samples taken. (X-ray crystallography)

f) Thus to determine the dominant wear mechanisms and discuss their underlying causes.

Chapter 2

Literature Survey

This literature survey is carried out to study and evaluate the wear properties of Al-Sn alloys. The various parameters like Sn content, applied load, angle of impingement, sliding distance, effect of microstructure etc. have been studied. For background information, the work of researchers in this respect has been considered. Some of their conclusions are as follows:

Chandi Prasad Mohanty and **Vicky Vikram Das (2011)** have studied the wear behavior of Al-Si alloys. They have taken samples of these alloys and performed wear tests like abrasive wear test and lubricated wear test. The variables involved in their wear test were normal load applied, % Si content in the alloy samples taken, sliding velocity, sliding distance and lubrication.

From the Vickers's hardness test, they found that hardness values are found to increase with increase in Silicon content in the alloy. They arrived at conclusions that with increase in applied load and sliding speed, wear is observed to increase. However, it was discovered that with increase in the % of Silicon in the alloy composition, wear rate reduces and cumulative mass loss decreases. Their most intriguing result is that the specimens showed higher amount of loss of material i.e. higher rate of wear under lubricated conditions for reasons unknown.

They expected that this behavior may be due to the easy removal of precipitated silicon platelets from the material due to easy interaction of Al-Si eutectic and silicon platelets (i.e.pro-eutectic silicon) at the inter boundary zone and thus material loss got enhanced.

Pratyasha Mohapatra and Swayam Prakash Sahoo (2013) have studied the erosive wear behavior of Aluminium-3 Magnesium-10 Silicon Carbide composites. Samples of these composites were taken and erosion wear test was performed. The effect of process parameters like impingement angle, impingement velocity, standoff distance on erosion wear rate was observed and analyzed.

From the graph obtained for Cumulative mass loss Vs erosion time for angle of impingement 90º, they observed that during initial stages of erosion there is sharp increase in mass loss for the initial 2mins after which the rate of mass loss became sluggish followed by steady increase in mass loss at a constant rate. They comprehended that the reason for this may be due to the fact that during

initial stages, erosion rate is rapid as the material is soft but after bombardment for a longer period the surface of the material gets hardened due to which wear rate slows down. With further progress of time, porous regions may develop on surface or tearing of grains on surface may occur leading to the increase again.

They observed that erosion rate decreases with increase of angle of impingement irrespective of the velocity of bombardment. Further it is maximum at an angle of 30º and decreases with increase in angle finally becoming minimum at an angle of 90º.It was deciphered that as erosion rate is higher at lower angles , it occurs by ductile mechanism. For brittle materials wear rate is maximum at an angle of 90º. From the reference provided in their work, it will be known that tangential and normal components of the velocity of erodent particles may be resolved and they separately influence wear properties. The plastic deformation of the composite is brought about by the tangential velocity component and at lower angles of impingement, the tangential velocity component is of higher magnitude. This is the reason why it was said that at lower angles wear occurs by ductile mechanism. For the samples taken by them, since erosion wear rate was observed to be greater at lower angles, erosion behavior was considered ductile.

It was observed that erosion rate increased with increase in impingement velocity. This is because as impingement velocity increases, momentum and kinetic energy of the striking particles also becomes greater. As the standoff distance increased, erosion rate was observed to decrease. This was because as standoff distance increased, the erodent particles travelled a longer path before striking the surface of the samples taken. Because of this, particles lose much of their energy.

Tuti Y. Alias and M.M Haque [5] have studied the wear behavior of as-cast and heat treated Al-Si eutectic alloys. Wear tests on the alloy samples taken were performed on a pin on disk type wear testing apparatus. The process parameters were size and shape of the pin, speed, load and the material.

With increase in the rotational speed of the disk, mass loss of the as –cast and heat treated alloys was observed to increase. The as –cast samples. High speed leads to reduction in wear rate. The reduction is pronounced in heat treated samples. This is because during sliding, heat is developed

and the material becomes softer and weaker. This heat might not affect the hardness of heat treated alloys due to their inherent characteristics.
Increase in the applied load leads to a high wear rate for both as –cast and heat treated alloys. But at higher loads, strain-hardening of the materials in contact increases, resulting in increase in the resistance to abrade or erode. At higher load, real surface area in contact is more which increases the gripping action and due to which wear rate slows down.

At longer sliding distances, volumetric wear rate and specific wear rate are low. This was attributed to the fact that during sliding, heat develops due to friction which makes some of the adhered materials soften and loosen. As sliding goes on, these loosened particles are thrown away showing higher loss in weight. Heat treated alloys are not much affected due to their inherent characteristics due to heat treatment cycles whereas as cast alloys show higher weight loss.

H. Torabian, J.B Pathak and S.N Tiwari [6] have studied the effects of alloy composition, sliding distance, sliding speed and load on the wear rate of Al-Si alloys.

The wear rate depends on the applied load. It has linear relationship with the load. Mild wear, Intermediate wear and severe wear are the three types of wear that happen in an alloy. Low loads lead to mild wear which takes a longer duration and takes place under low loads. The intermediate wear and severe wear regions are distinguished from the mild region by higher rates of increase in the wear rate per unit weight.

It may be observed that the transition load at which change takes place from one region to another increases with increased Silicon content of the alloy. It is observed that wear rate initially decreases slightly with increasing sliding speed up to a certain value. Beyond this, there is a sharp rise in the wear rate, irrespective of the alloy composition. This value increases with increasing Silicon content.
The wear rate of the alloy is strongly dependent on the Silicon content of the alloy. The wear rate is found to decrease with increasing Silicon content. This effect is pronounced upto 15% Si in the alloy. Thus wear rates of hypereutectic alloys are better than those of hypoeutectic alloys.

K. Lepper , M. James , J. Chashechkina ,and D.A. Rigney [4] have studied the sliding behavior of some selected aluminium alloys. This project was undertaken to achieve three principal objectives: to improve understanding of the behavior of selected aluminium-based hearing materials used in sliding applications, to develop improved guidelines for the design of such beatings and to respond to increasing environmental concerns about the use of lead in heating materials.

Unlubricated sliding tests have been conducted using disks of Al-Sn and Al-Pb binary alloys as well as multicomponent alloys produced with the aid of an MHD (magneto hydrodynamic) technique at the Institute for Solid State Physics, Chemogolovka. Russia. For comparison, commercial alloys produced by Glacier Vandervell Inc. have also been tested. The counterface in each case was a hardened 52100 ball. Sliding speeds were kept low (1530 mm s-‘) to limit frictional temperature increases.

Normal loads ranged from 0.8 to 1.2 kgf. Earlier results on Pb-Sn and Babbitt alloys demonstrated that the environment strongly affects the friction coefficient, the smoothness of sliding and the hardness and hardness gradient at the surface. Therefore we have performed tests in vacuum (as a reference condition) and in air. A range of complementary techniques (optical and electron microscopy, X-ray fluorescence analysis using energy dispersive spectroscopy (EDS), microhardness) was used for structural and chemical characterization of debris and of surface and near-surface material.

In all cases, sliding in vacuum was smooth and the wear rates were low. In fact, the rate of production of debris during the vacuum tests was negligible. However, the friction coefficient, the fluctuations in friction and the wear rate were all much higher for tests in air. The reasons for this behavior are associated with dramatic differences in structure and composition which develop near the surface of the bearing material. The effects of environment are larger than those associated with changes in composition for the alloys Studied.

Chapter 3

Experimental Details

3.1 Sample preparation

Aluminium was melted in a pit furnace with graphite crucibles. Initially Al was melted and then tin pieces wrapped in an Aluminium foil are added. The melt was stirred with a graphite rod and then casted in a graphite mould. The Aluminium melted was of commercial purity (98 %). The composition was Al-99% and Sn-1%.

Sample sizes of 22mm X 22mm X 6mm were cut .The surface of the cut samples were irregular and rough. So belt grinder was used to make it regular. Emery papers of 1/0, 2/0, 3/0 and 4/0 grades was used to polish the surface and diamond polisher was used to get mirror type finish on the sample surface. The prepared samples were then proceeded for various tests.

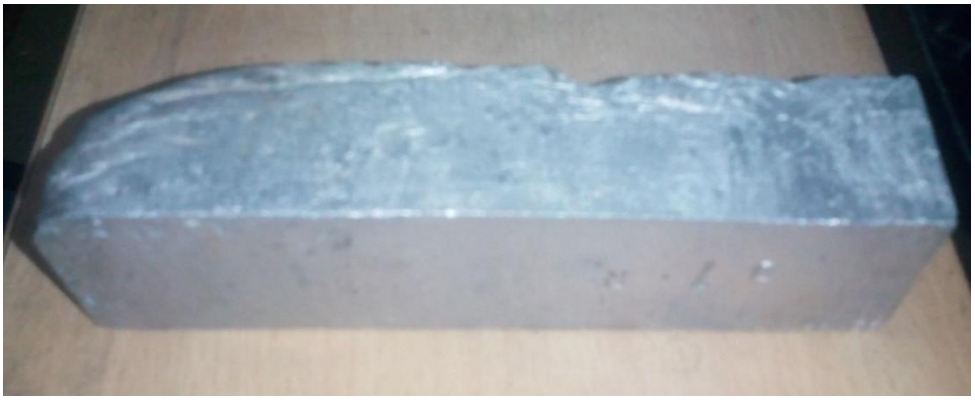

Fig 7: Prepared As-cast Al-1%Sn alloy sample

3.2 Hardness Measurement

Hardness test of the sample was done using a Vickers' Micro Hardness Tester. The HV number is determined by the ratio F/A, where F is the force applied to the diamond in kilograms-force and A is the surface area of the resulting indentation in square millimeters. A can be determined by the formula,

$$A = \frac{d^2}{2\sin(68^\circ)}$$

Which can be approximated by evaluating the sine term to give

$$A \approx \frac{d^2}{1.8544}$$

Where d is the average length of the diagonal left by the indenter in millimeters. Hence

$$HV = \frac{F}{A} \approx \frac{0.1891F}{d^2}$$

Where F is in N and d is in millimeters. Here, HV is in GPa and should be roughly between 0-15 GPa.

When doing the hardness tests the minimum distance between indentations and the distance from the indentation to the edge of the specimen must be taken into account to avoid interaction between the work-hardened regions and effects of the edge.

The Load applied is 10gf and the dwell time is 10seconds.

Fig 8: Vickers' Micro Hardness Test Setup

3.3 Optical Microscopy

The perfectly grinded and polished samples were then imaged under Zeiss optical microscope. Magnifications involved were 5x, 10x, 20x and 50x.

Fig 9: Zeiss Optical Microscope

3.4 XRD analysis

The phases present in the prepared samples were analyzed by Bragg- X-ray diffraction (XRD) using Cu Kα (λ=0.15406 nm) radiation in a Philips X-ray diffractometer.

The Experimental procedure involved three main steps.

- The first and most difficult step is to get the sample crystal which was sufficiently large (greater than 0.1mm all dimensions), had high purity composition and had regular structure, without having any significant internal imperfections like twinning or cracks.

- The second step involved placing the sample in an intense beam of X-rays, usually of single wavelength (monochromatic X-rays), so that a regular pattern of reflections are produced. As the crystal rotates gradually, previous reflections disappeared and new ones appeared; the intensity at every orientation of every spot was recorded. Collection of multiple data

sets was required, with each set covering more than half a full rotation of the crystal and containing typically tens of thousands of reflections.

- In third step, the data obtained was combined computationally with complementary chemical information to produce and refine a model of arrangement of atoms within the crystal. Finally an Intensity Vs 2Θ Plot was obtained showing all the diffraction peaks.

3.5 Erosion wear

The Air Jet Erosion Test Rig machine is used for testing the erosion resistance of solid materials when erodent particles under desired pressure are impinged into the solid material. The test is conducted as per ASTM G76 standards. This test can be conducted over a wide range of particle sizes, velocities, incident angles and particle fluxes in order to generate quantitative data on the materials and study the mechanisms of damage.

Fig 10: Erosion wear test setup

3.5.1 Test Apparatus

Fig 11 shows the schematic figure of the erosion wear test apparatus. The erosion wear testing rig consists of an air compressor, an air drying unit, a magnetic particle feeder, an air-particle mixing and accelerating chamber. A compressor is used to compress the air which has maximum compressing capacity of 12 bar. The compressed air gets mixed with the particles after it is let into the erosion wear testing rig. The erodent particles are fed at a constant flow rate from a conveyor belt type feeder present in the mixing chamber. The erodent particles are then accelerated through a converging nozzle having 4 mm diameter. These accelerated particles impinge the specimen. The specimen can be held at various angles with respect to the impinging particles with the help of an adjustable sample holder. The distance between the belt and the particle feeding hopper is adjusted to control the feed rate of the particles. Pressure of the compressed air can be varied to change the impact velocity of the erodent particles. The erodent used here is dry silica sand. Some of the features of this test set up are:

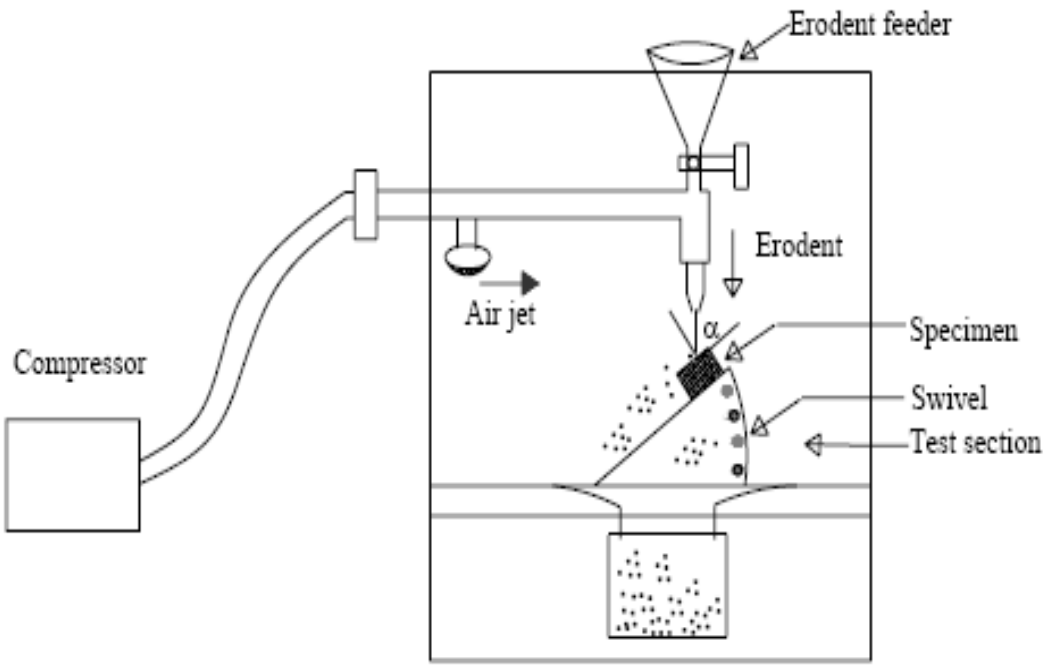

Fig 11: Schematic diagram of Erosion Wear test rig

The various parameters for this test are as follows:

Erodent	Silica sand
Erodent size (µm)	400
Impingement angle α (⁰)	30, 45, 60, 90
Impact velocity (m/s)	48,82,109
Erodent feed rate (g/min)	12
Test temperature	RT
Nozzle to sample distance (mm)	20
Nozzle diameter (mm)	4

Table 1: Parameters of Erosive Wear Test

3.5.2 Experimental procedure

1. Acetone was used to clean the prepared samples which were dried after that and their initial weight was measured using electronic balance.

2. The sample was eroded at different impact angles (30, 45, 60, and 90) for total 10mins during which after every 2min interval the weight was measured.

3. A precision electronic balance with 0.001 mg accuracy was used to calculate the weight loss. Erosion rate was calculated as the ratio of the weight loss to the weight of the eroding particles.

4. The damages in the surfaces were then characterized by SEM.

3.6 Sliding Wear

Wear resistance of the Al-Sn and pure Al samples was evaluated using a ball on plate type wear testing instrument having a diamond indenter at room temperature. DUCOM TR-208-M1 ball on plate wear tester was used.

Fig 12: Ball on plate wear test Setup

3.6.1 Experimental Procedure

1. The samples were fixed in a circular base of the DUCOM TR-208-M1 ball on plate wear tester.

2. Various parameters like track diameters (4mm, 8mm, 12mm) and loads (10N, 20N) were provided to the machine.

3. Different times (5min, 15min, 20min) and different RPM's (10, 20, 25, 30) was also set.

4. The wear depth vs time data was obtained from the inbuilt WINCOM software in the wear machine. The damages in the surfaces were characterized by SEM.

3.7 Corrosive Wear

Corrosion resistance of the prepared samples was done by placing the samples in a small beaker. The beaker was filled with sea water that would facilitate corrosion easily. Weights of the corroded sample was taken after one day, one week, two weeks and 4weeks during the test process of 4weeks.

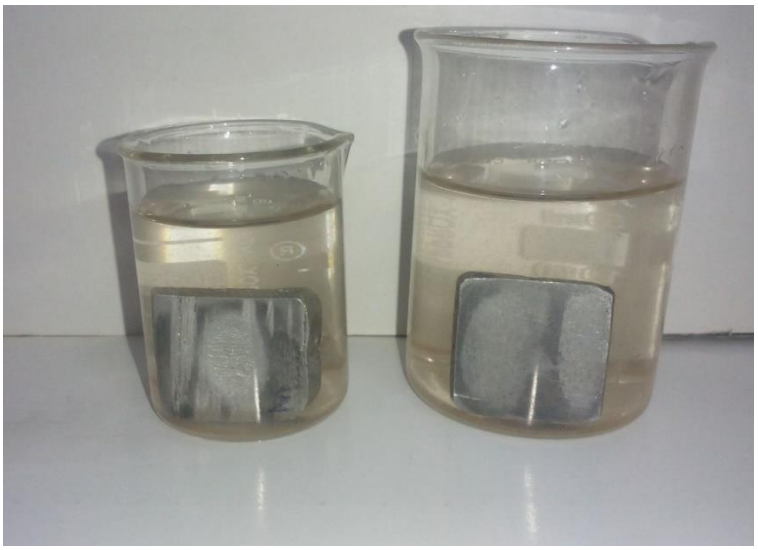

Fig 13: Samples under Corrosion test

3.8 SEM

The sample after erosion wear, the sample after sliding wear and the sample after corrosive wear were studied by JEOL JSM-6480 LV scanning electron microscope(SEM) having high energy X-Ray detector.

Fig 14: Scanning Electron Microscope Setup

Chapter 4

Results and Discussions

4.1 Microstructure

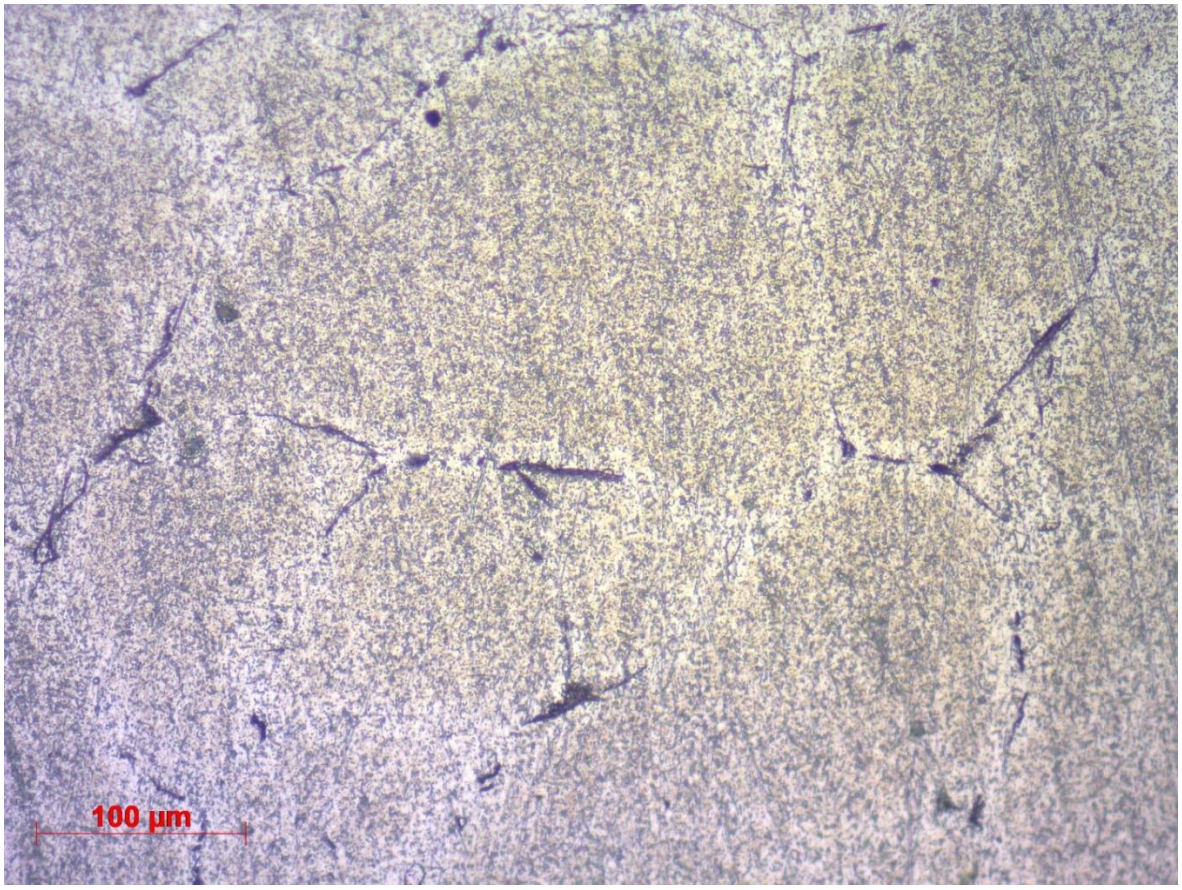

Fig 15: Micrograph of As-cast Al-1%Sn alloy sample

As per the above micrograph, the dark particles present in it is tin which is almost homogeneously distributed in the matrix of aluminium. The grain boundaries can also be viewed.

4.2 Hardness Measurement

- Pure Al Sample

Length of diagonal D1(μm)	21.13	20.58	18.77
Length of diagonal D2(μm)	19.34	20.07	19.87
Vickers's Hardness Value (HV)	45.3	44.91	49.7

Table 2: Hardness values at 3 different positions in the pure Al sample

The average value of Vickers's hardness value of the pure Al came to be 46.63HV.

- As-cast Al-1%Sn alloy

Length of diagonal D1(μm)	21.76	22.00	21.18
Length of diagonal D2(μm)	22.70	21.86	23.03
Vickers's Hardness Value (HV)	93.70	96.4	94.9

Table 3: Hardness values at 3 different positions in the As-cast Al-1%Sn sample

The average value of Vickers's hardness value of the As-cast Al-1%Sn alloy came to be 95.01HV.

So comparing the two table, it can be said that the hardness of alloy sample is more than the purer one. This is because alloys contain atoms of different sizes, which distort the regular arrangements of atoms. Thus the sliding of layers over each other becomes more difficult.

4.3 XRD Analysis

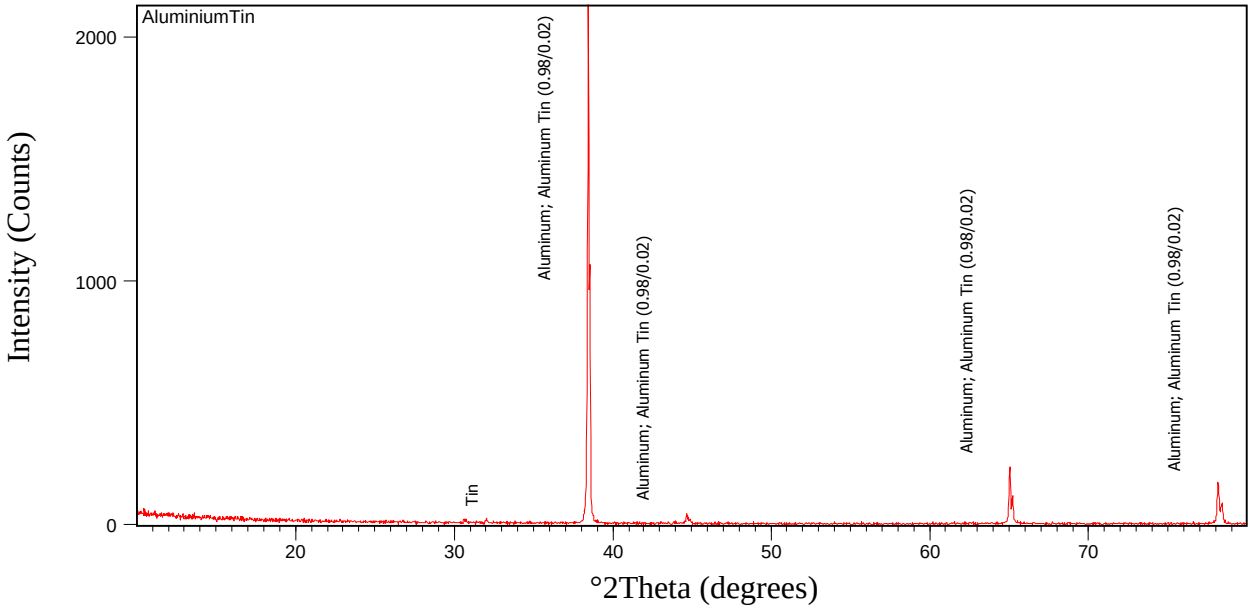

Fig 16: Intensity vs 2Theta for As-cast Al-1%Sn alloy sample

The XRD plot of the sample shows the presence of different phases. Tin phase, aluminium phase and both the tin and aluminium phases are present at various positions in the sample.

4.4 Erosive Wear

- Lowest Velocity (2 bar pressure):

Angle(degrees)	30	45	60	90
Initial weight of Sample(g)	7.228	8.563	7.067	5.741
Weight after 2mins(g)	7.227	8.562	7.066	5.740
Weight after 4mins(g)	7.223	8.559	7.065	5.738
Weight after 6mins(g)	7.222	8.557	7.064	5.737
Weight after 8mins(g)	7.221	8.553	7.061	5.733
Weight after 10mins(g)	7.220	8.552	7.059	5.732

Table 4: Weight values after every 2mins for different angles at 48m/s for the As-cast Al-1%Sn alloy sample

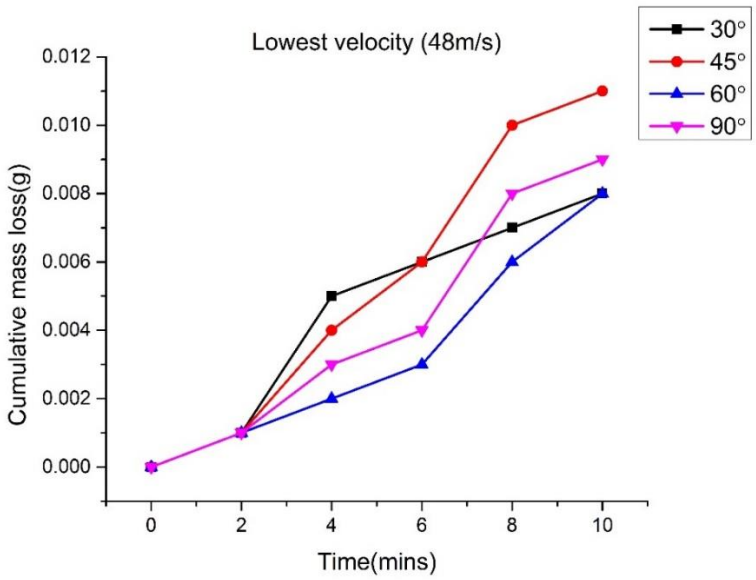

Fig 17: Cumulative mass loss vs Time for the As-cast Al-1%Sn alloy sample at 48m/s

As per Fig 17, maximum cumulative loss occurred for the impingement angle of 30^{θ} and minimum for the impingement angle of 60^{θ}.

- Medium Velocity (3 bar pressure):

Angle(degrees)	30	45	60	90
Initial weight of Sample(g)	8.613	7.114	5.963	5.733
Weight after 2mins(g)	8.604	7.104	5.950	5.731
Weight after 4mins(g)	5.593	7.098	5.939	5.727
Weight after 6mins(g)	8.583	7.089	5.934	5.725
Weight after 8mins(g)	8.572	7.081	5.928	5.722
Weight after 10mins(g)	8.564	7.067	5.923	5.719

Table 5: Weight values after every 2mins for different angles at 82m/s for the As-cast Al-1%Sn alloy sample

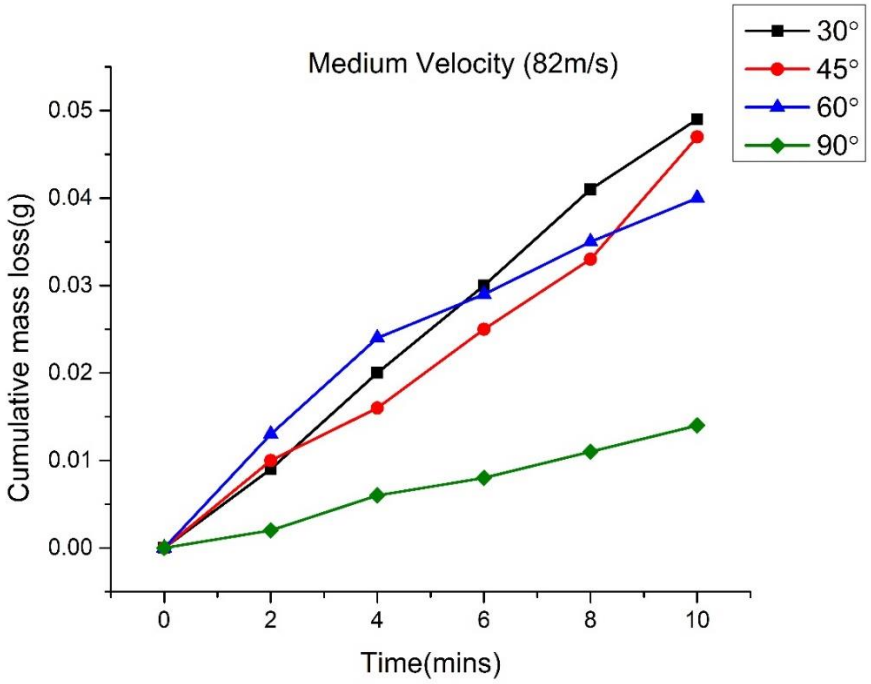

Fig 18: Cumulative mass loss vs Time for the As-cast Al-1%Sn alloy sample at 82m/s

As per Fig 18, maximum cumulative loss occurred for the impingement angle of 30^{θ} and minimum for the impingement angle of 90^{θ}.

- Highest Velocity (4 bar pressure):

Angle(degrees)	30	45	60	90
Initial weight of Sample(g)	7.224	4.043	6.006	6.149
Weight after 2mins(g)	7.208	4.042	5.997	6.147
Weight after 4mins(g)	7.195	4.033	5.987	6.141
Weight after 6mins(g)	7.181	4.027	5.977	6.136
Weight after 8mins(g)	7.168	4.020	5.968	6.131
Weight after 10mins(g)	7.151	4.009	5.963	6.126

Table 6: Weight values after every 2mins for different angles at 109m/s for the As-cast Al-1%Sn alloy sample

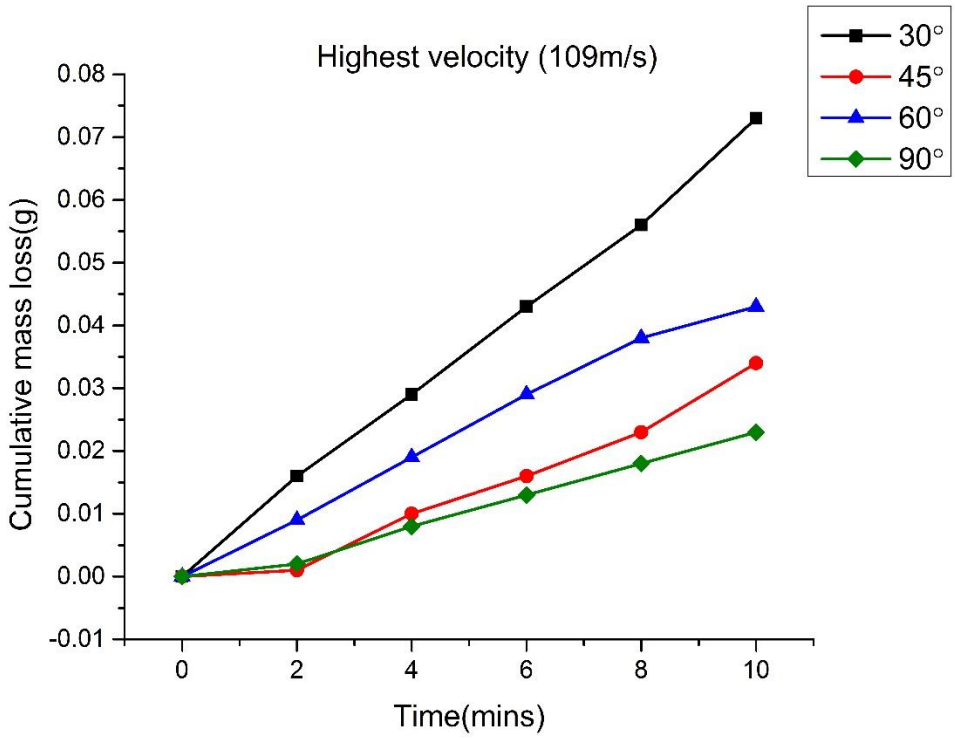

Fig 19: Cumulative mass loss vs Time for the As-cast Al-1%Sn alloy sample at 109m/s

As per Fig 19, maximum cumulative loss occurred for the impingement angle of 30^{θ} and minimum for the impingement angle of 90^{θ}.

For the figures 17, 18 and 19, at the initial stage of corrosion i.e. upto 2mins, there is a sharp increase in the mass loss. Then the rate of mass loss becomes less from 2 to 6mins. The erosion is high at the initial stage because the material is soft. But after impingement of erodent particles for longer duration, the material surface gets hardened for which the material loss rate is less. The rate of mass loss increases still after 6mins may be due to the tearing of grains and development of porous regions on the surface.

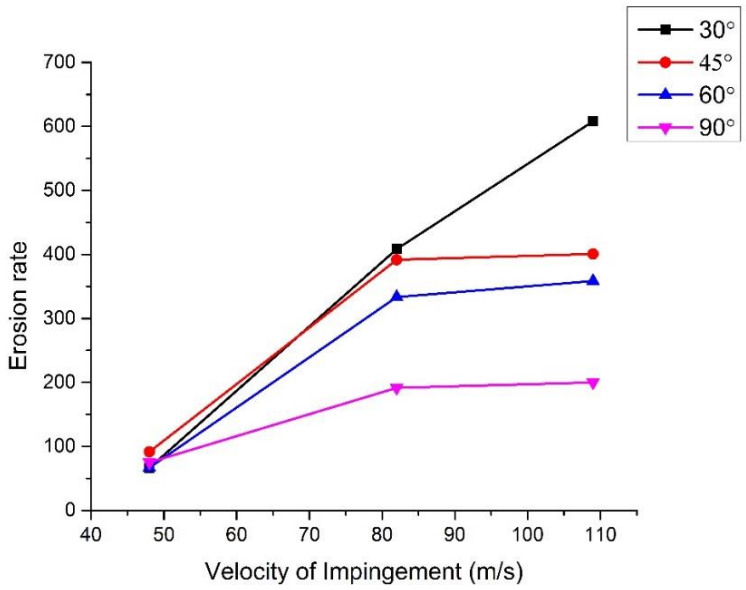

Fig 20: Erosion rate vs Velocity of Impingement for As-cast Al-1%Sn alloy sample

Fig 20 shows that the erosion rate increases with the increase in the impingement velocity. The higher is the impingement velocity, the greater is the momentum and kinetic energy carried by the particles striking the surface which leads to greater erosion rate. The erosion rate at 30^0 is seen to be highest as compared to other angles.

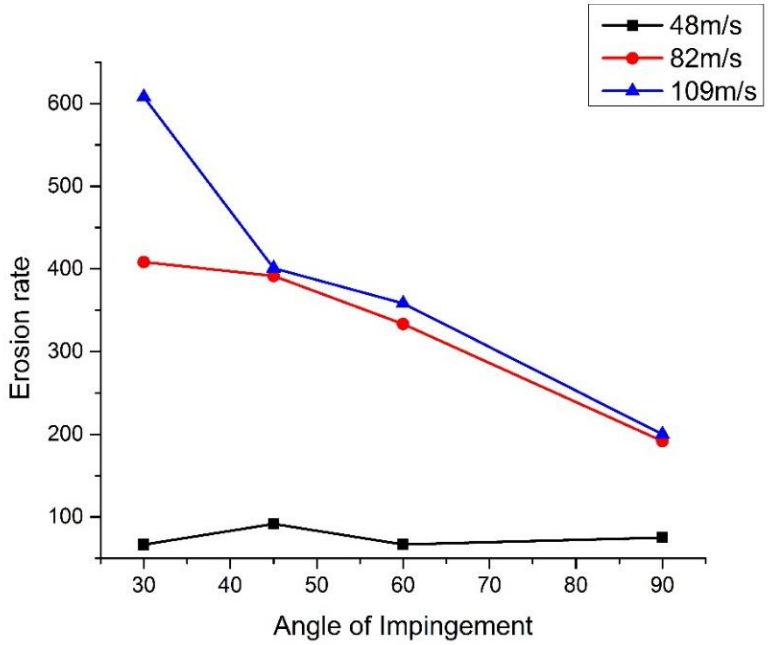

Fig 21: Erosion rate vs Angle of Impingement for As-cast Al-1%Sn alloy sample

Figure 21 shows that the erosion rate decreases with the increase in the angle of impingement. The erosion wear rate is highest at lower angle of impact i.e. at 30^{θ} and lowest at higher angle of impact i.e. 90^{θ} angle. It can be said that the erosion occurs by ductile mechanism as the maximum erosion occurs at lower angles, Rattan [9] has studied the effect of the angle of impingement on the solid particle erosion rate and suggests that erosion of ductile materials is maximum at an angle of impingement in the range of 15^{θ} to 30^{θ} while erosion of brittle materials is maximum at 90^{θ}.

Ibrahim [10] studied the relationship of the impingement angle on the mechanism of erosion wear. He stated that the tangential and normal components of velocity of the erodent particles can be separated which control the wear mechanism. When particles strike the sample surface at a particular angle, the tangential component of particle velocity leads to plastic deformation of the material. Lower is the impingement angle, greater is the tangential component of the velocity; thus greater is the wear by plastic deformation. Thus the erosion rate of the material is higher at lower angles which suggests erosion behavior is ductile in nature [11].

Bayer [12] studied the relationship between the impact angle and the erosion rate in relation to ductile and brittle materials. Bayer suggested that the ductile nature is prominent at lower angles of 20^{θ} to 30_{o} while brittle nature of erosion is prominent at higher angles (90^{θ}). The two main mechanisms i.e. micromachining and ploughing mechanism leads to erosion. At lower impact angles the erodent particles strike the surface and cause maximum erosion by forming grooves as they slide across the ductile surface [13].

4.5 Sliding Wear

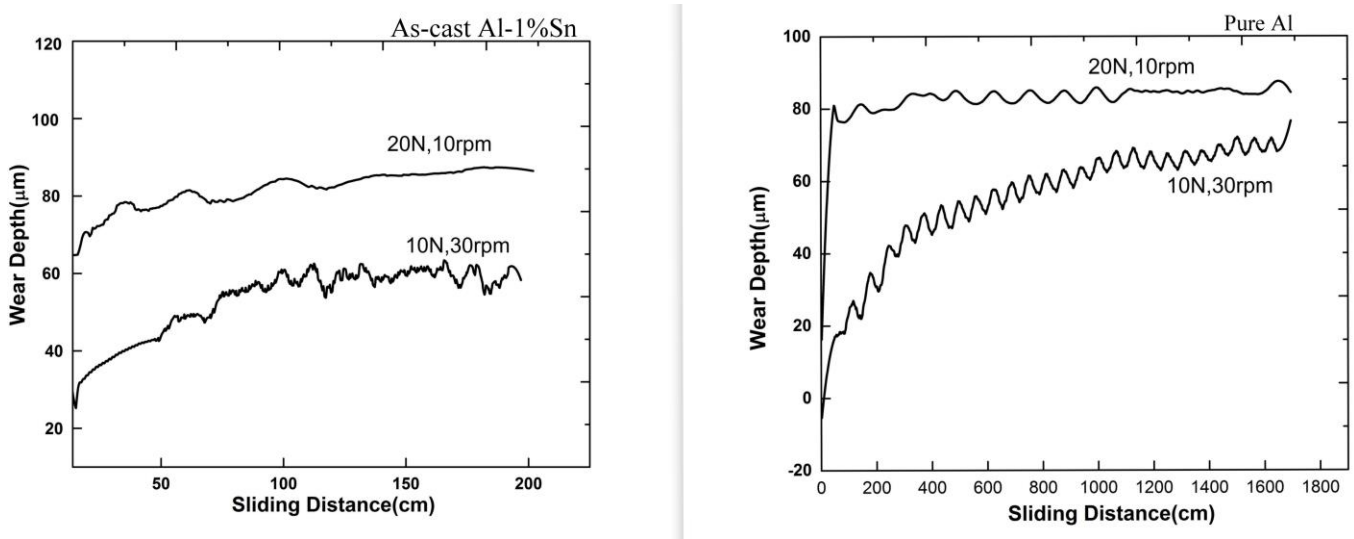

Fig 22: Wear depth vs Sliding Distance of As-cast Al-1%Sn and Pure Al operated for a time of 15mins in the Ball on Plate Wear tester

Fig 22 shows that the amount of wear is mostly dependent on load applied. So greater the load, more is the wear depth. For a particular load and rpm applied, the wear depth of the As-cast Al-1%Sn alloy sample is less than that of pure Al sample.

4.6 Corrosive Wear

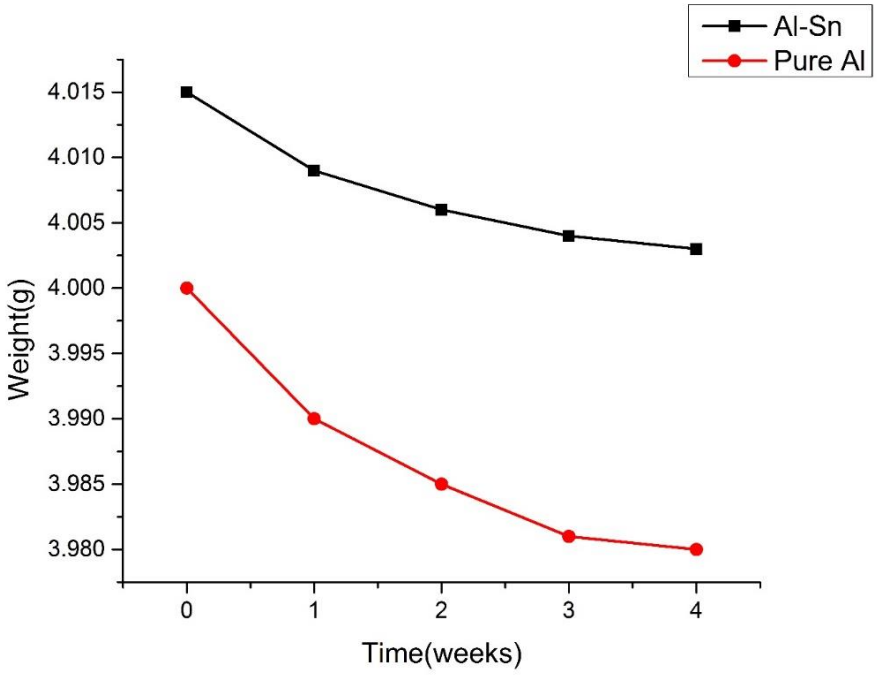

Fig 23: Weight vs Time for As-cast Al-1%Sn alloy and pure Al sample both after Corrosive wear

As per Fig 23, it seems that the rate of corrosion of alloy sample is less than that of pure sample. This is because the addition of tin reduces the corrosion of the alloy sample. Tin having greater ductility than aluminium reduces the susceptibility of corrosion in the alloy sample.

4.7 SEM Analysis

- Corrosive wear fractographs

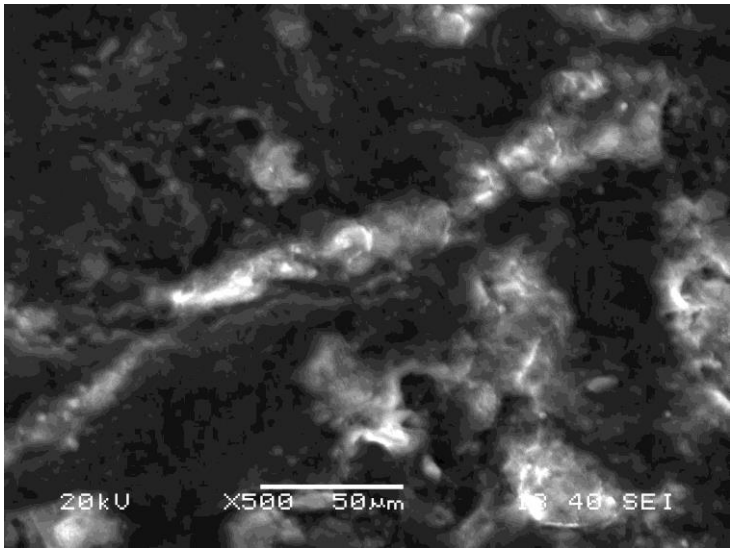

Fig 24: Fractograph of As-cast Al-1%Sn Alloy sample after 1 week of Corrosive wear

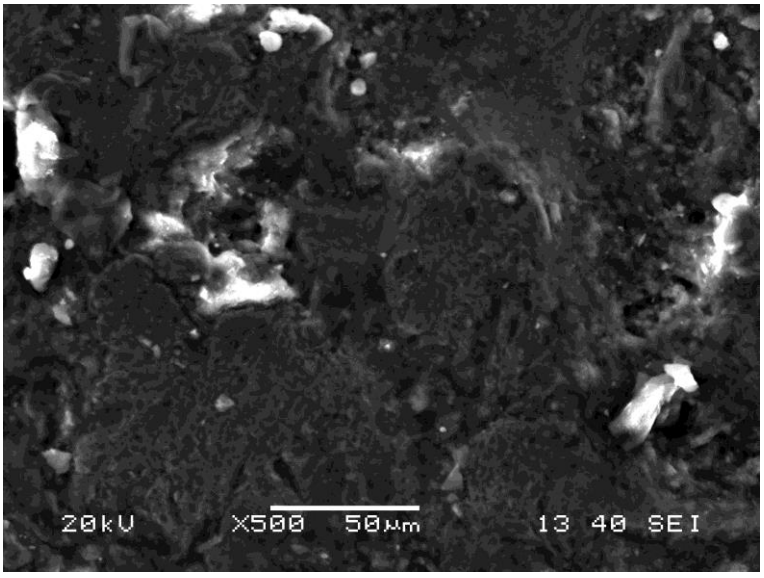

Fig 25: Fractograph of Corrosive wear As-cast Al-1%Sn Alloy sample after 2weeks of Corrosive wear

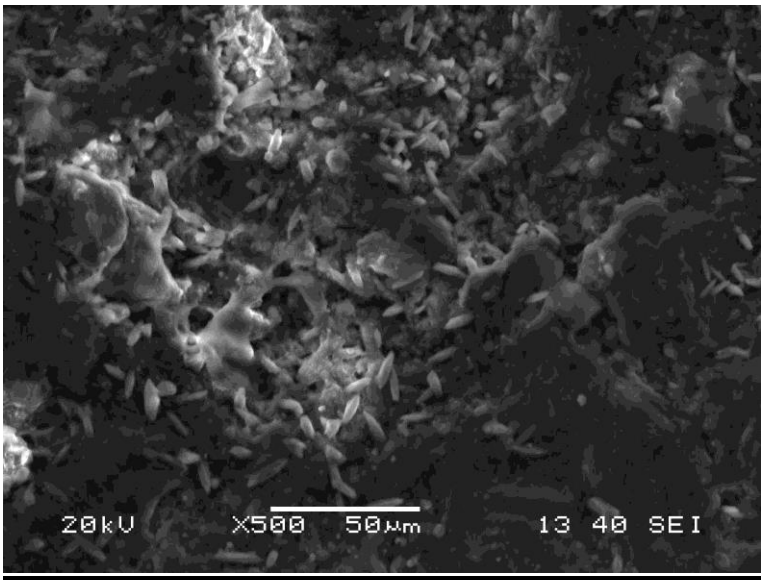

Fig 26: Fractograph of Corrosive wear As-cast Al-1%Sn Alloy sample after 4weeks of Corrosive wear

Fig 24,25 and 26 shows the difference in the fractographs of th As-cast Al-1%Sn alloy sample. More is the time of corrosion, more will be the corrosion effect on the sample surface which can be seen through the fractographs i.e. more corrosion for 4weeks of test and less for 1 week of test.

- Erosive wear fractographs

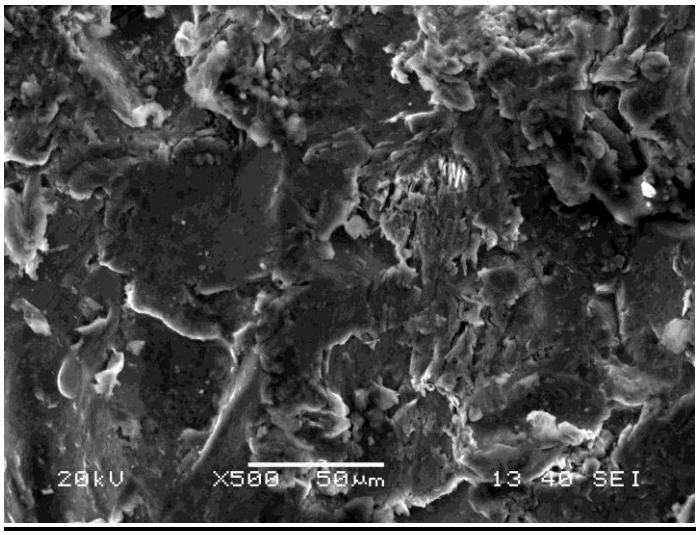

Fig 27: Fractograph of As-cast Al-1%Sn Alloy sample at an impingement angle of 30^0 after erosion wear

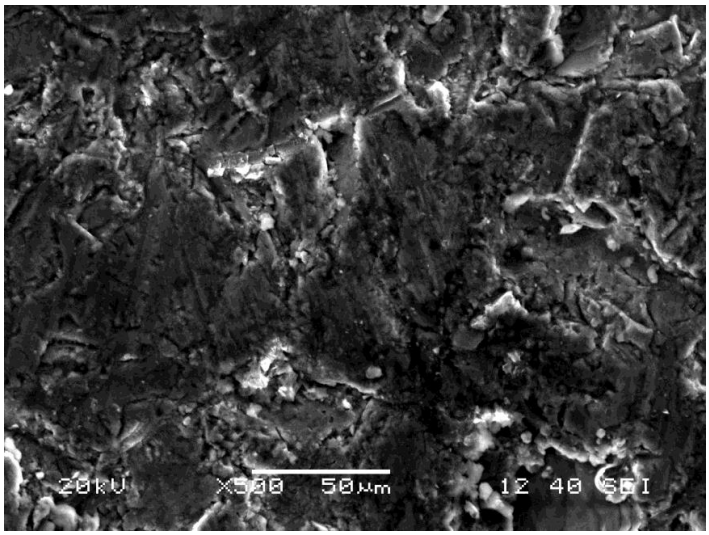

Fig 28: Fractograph of Eroded As-cast Al-1%Sn Alloy sample at an impingement angle of 45^{θ} after erosion wear

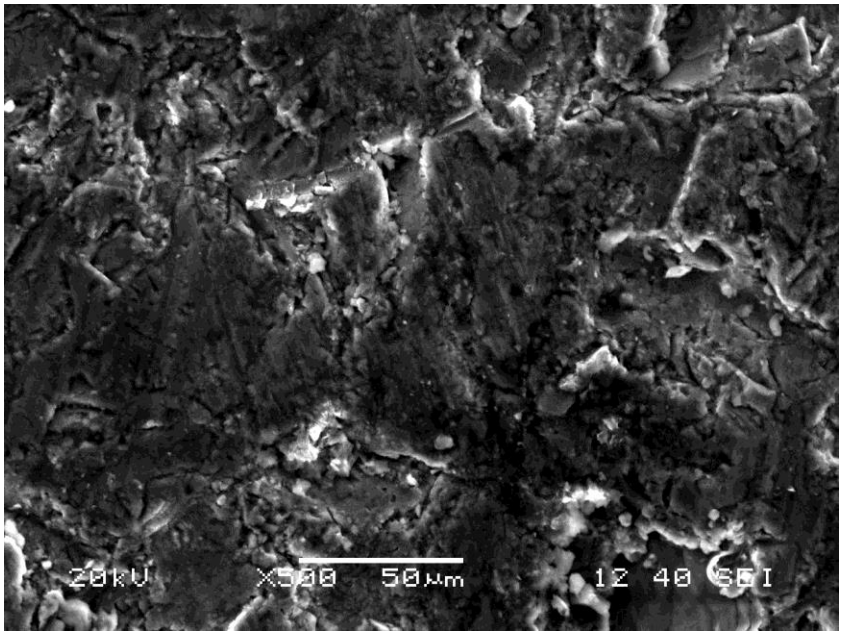

Fig 29: Fractograph of Eroded As-cast Al-1%Sn Alloy sample at an impingement angle of 60^{θ} after erosion wear

From the fractographs of fig 27,28 and 29, it can be seen that intergranular cracks have occurred. Ploughing of particles is more for less angle of impingement i.e. 30^{θ}.

- Sliding wear fractographs

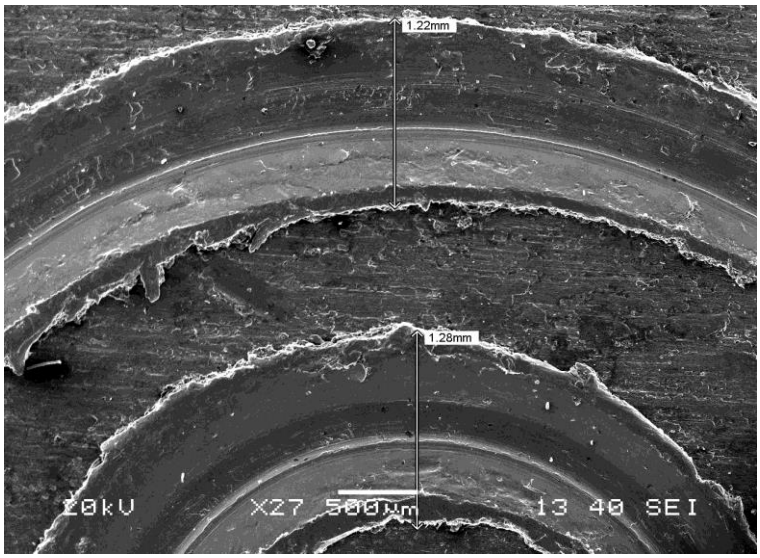

Fig 30: Fractograph of tracks of As-cast Al-1%Sn Alloy sample for 5mins(top) and 15mins(bottom) at 10rpm and 20N load after sliding wear

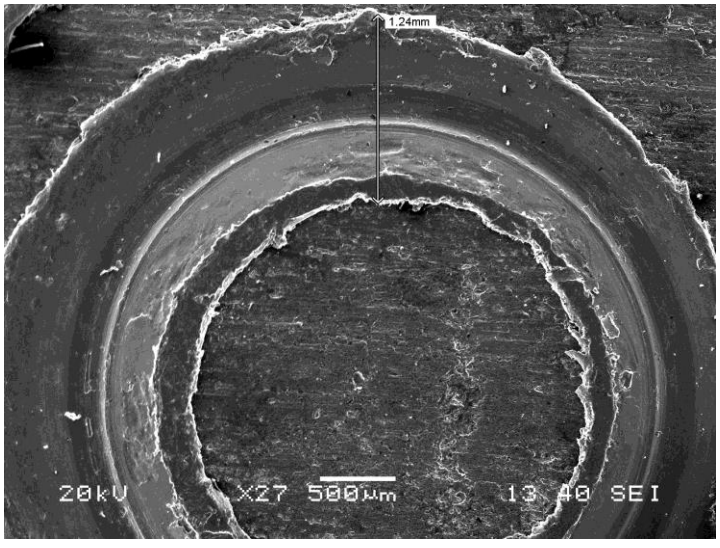

Fig 31: Fractograph of tracks of As-cast Al-1%Sn Alloy sample for 10mins at 10rpm and 20N load after sliding wear

From the fig 30 and 31, it can be observed that more is the time of sliding wear, more is the length of the track observed on the surface of sample i.e. 1.22mm for 5mins of test,1.24mm for 10mins of test and 1.28mm for 20min of test. This is because more is the time of the diamond indentor sliding over the surface, more material from the surface will be pushed away from the centre.

Chapter 5

CONCLUSION

- Hardness value of the As- cast Al-1%Sn alloy sample was higher than that of pure Al alloy.
- Corrosion rate of the As-cast Al-1%Sn alloy was found to be less than that of pure Al.
- The wear depth of the As-cast Al-1%Sn alloy sample was observed to be less than that pure Al for a given load, time and rpm.
- Since cumulative weight loss of As-cast Al-1%Sn is maximum at lower impact angles, it can be inferred that wear mechanism is ductile in nature.

Thus it can be concluded that the As-cast Al-1%Sn alloy sample can be used as bearing materials in automotive industries due to its superior wear resistant behaviour.

Scope for future work

We have performed the test for the alloy samples with 1% Tin composition. Not many tests have been performed with these alloys so far. So further investigations with varying tin compositions can be performed. Accordingly applications may be obtained depending on the corresponding properties.

Chapter 6

REFERENCES

[1] Tomasz Stuczynski, "Metallurgical problems associated with the production of aluminium-tin alloys", Institute Non-Ferrous Metals, August 1997.

[2] Dr.Eman J. Abed, "Study of Solidification and Mechanical Properties of Al-Sn Casting Alloys", Dept. of Materials Engineering University of Kufa, July 2012.

[3] www.freepatents.com

[4] www.inference.phy.cam.ac.uk

[5] Tuti Y. Alias and M.M. Haque, Wear properties of aluminium silicon eutectic Alloy, Icme03-am-151 ©, 2003.

[6] Torabian H, Pathak JP and Tiwari SN, "Wear characteristics of Al-Si alloys", Wear, Volume 172, pages 49-58, 1994.

[7] W. Carrick Anderson and George Lean, "The Properties of The Aluminiuim-Tin Alloys", Proceedings of the Royal Society of London, Vol, page 277- 284, 1903.

[8] K. Lepper , M. James , J. Chashechkina , D.A. Rigney, "Sliding behavior of selected Aluminum alloys", Wear 203-204, page 46-56, 1997.

[9] Rattan,Jayashree Bijwe, "Influence of impingement angle on solid particle erosion of carbon fabric reinforced polyetherimide composite", Sci. Technol. Adv. Mater.8, 2002.

[10] A.T Ibrahim," A mechanisms for solid particle erosion in ductile and brittle materials", MS Thesis, Wichita State University, 1990.

[11] K.V.Pool, C.K.H.Dharan and I.Finnie,"Erosion Wear of Composite Materials", Sci. Technol. Adv. Mater. 9, 033002, 2008.

[12] Bayer G,"Mechanical Wear Prediction and Prevention" – Marcel Dekkar, Inc., New York: page 396, 1994.

[13] A. Alahelisten, P. Hollman and S. Highmark, "Solid Particle Erosion of Hot Flame Deposited Diamond Coatings on Cemented Carbide", Volume 117, page 159-165, 1994.